Journal of Power Sources 184 (2008) 489–493

Contents lists available at ScienceDirect

Journal of Power Sources

journal homepage: www.elsevier.com/locate/jpowsour

Short communication

High power and high capacity cathode material $LiNi_{0.5}Mn_{0.5}O_2$ for advanced lithium-ion batteries

Xianglong Meng, Shumei Dou, Wen-lou Wang*

Department of Chemical Physics, The University of Science and Technology of China, Hefei, Anhui 230026, PR China

ARTICLE INFO

Article history:
Received 8 January 2008
Received in revised form 2 April 2008
Accepted 8 April 2008
Available online 14 April 2008

Keywords:
$LiNi_{0.5}Mn_{0.5}O_2$
Lithium-ion battery
Solid reaction
$Ni_{1.5}Mn_{1.5}O_4$
Precursor

ABSTRACT

Single-phase lithium nickel manganese oxide, $LiNi_{0.5}Mn_{0.5}O_2$, was successfully synthesized from a solid solution of $Ni_{1.5}Mn_{1.5}O_4$ that was prepared by means of the solid reaction between $Mn(CH_3COO)_2{\cdot}4H_2O$ and $Ni(CH_3COO)_2{\cdot}4H_2O$. XRD pattern shows that the product is well crystallized with a high degree of Li–M (Ni, Mn) order in their respective layers, and no diffraction peak of Li_2MnO_3 can be detected. Electrochemical performance of as-prepared $LiNi_{0.5}Mn_{0.5}O_2$ was examined in the test battery by charge–discharge cycling with different rate, cyclic voltammetry (CV), and electrochemical impedance spectroscopy (EIS). The cycling behavior between 2.5 and 4.4 V at a current rate of 21.7 mA g^{-1} shows a reversible capacity of about 190 mAh g^{-1} with little capacity loss after 100 cycles. High-rate capability test shows that even at a rate of 6C, stable capacity about 120 mAh g^{-1} is retained. Cyclic voltammetry (CV) profile shows that the cathode material has better electrochemical reversibility. EIS analysis indicates that the resistance of charge transfer (R_{ct}) is small in fully charged state at 4.4 V and fully discharged state at 2.5 V versus Li^+/Li. The favorable electrochemical performance was primarily attributed to regular and stable crystal structure with little intra-layer disordering.

1. Introduction

During the past decade, rechargeable lithium batteries have been extensively investigated and widely used; they are not only required to enable the moderately charge/discharge rates applications like mobile phone and portable computer but also to meet an increasing need for new applications such as hybrid electric vehicles which need power sources with both high energy and high power density. Although the $Li_XC_6/Li_{1-X}CoO_2$ rechargeable batteries satisfy most of the requirements, the cost, toxicity and safety of cobalt have prevented their more widespread use. These limitations have stimulated investigation of alternative lithium-insertion electrodes [1–4].

Layered lithium nickel manganese oxides are promising, inexpensive and nontoxic alternative positive electrode materials to the commercial $LiCoO_2$ electrode used in lithium-ion batteries. Of these, $LiNi_{0.5}Mn_{0.5}O_2$ is one of the most attractive materials because it has about 280 mAh g^{-1} theoretical capacity [5–12]. Various synthesis methods, such as solid-state reaction [5–7], ion-exchange [7,12], hydroxide co-precipitation method [8,9], hydrothermal synthesis [10], ultrasonic assistance synthesis [11], etc., have been applied to prepare this material. However, it is difficult to obtain higher battery-active $LiNi_{0.5}Mn_{0.5}O_2$ due to either containing substantial Li/Ni disorder [7,12] or existing structural impurity [13] in $LiNi_{0.5}Mn_{0.5}O_2$. Recently, the major breakthrough in solving those problems is either to transform $Na(Ni_{0.5}Mn_{0.5})O_2$ into $Li(Ni_{0.5}Mn_{0.5})O_2$ by ion-exchange of Na^+ for Li^+ [7,12], or to use nickel manganese double hydroxides, i.e. one-to-one solid solution of $Ni(OH)_2$ and $Mn(OH)_2$ as precursor [5,6]. The former is a multi-step synthesis process, and needs to consume a large amount of salts containing Li^+. For the latter, it should be very careful to control the synthesis conditions in order to obtain the solid solution of $Ni(OH)_2$ and $Mn(OH)_2$ since Mn^{2+} in nickel manganese double hydroxides are easily oxidized in air when wet.

Nevertheless, it is a good idea to use the solid solution of $Ni(OH)_2$ and $Mn(OH)_2$ as the precursor instead of mixed hydroxides prepared by co-precipitation. The solid solution material is of the single phase, in which the distribution of Ni/Mn is homogeneous at atomic level, whereas, the mixed hydroxides are composed of particles with different phase. Therefore, electrochemical performance of $LiNi_{0.5}Mn_{0.5}O_2$ prepared from the solid solution of $Ni(OH)_2$ and $Mn(OH)_2$ is better than that prepared from the mixed hydroxides [5,6,8,9]. This stimulates our interest to explore a simple method to prepare the solid solution in order to obtain high battery-active cathode material. In this paper, we will report synthesis and characterization of higher battery-active $LiNi_{0.5}Mn_{0.5}O_2$ cathode material

* Corresponding author. Tel.: +86 551 3601117; fax: +86 551 3601592.
E-mail address: wlwang@ustc.edu.cn (W.-l. Wang).

0378-7753/$ – see front matter © 2008 Elsevier B.V. All rights reserved.
doi:10.1016/j.jpowsour.2008.04.015

prepared from the solid solution of $Ni_{1.5}Mn_{1.5}O_4$ with a very simple method. Comparing the solid solution of $Ni(OH)_2$ and $Mn(OH)_2$, the solid solution of $Ni_{1.5}Mn_{1.5}O_4$ is not sensitive to humidity and oxygen, and can be easily prepared. The as-prepared $LiNi_{0.5}Mn_{0.5}O_2$ from the solid solution of $Ni_{1.5}Mn_{1.5}O_4$ is of higher electrochemical reversibility, higher capacity (190 mAh g^{-1}), higher rate capability (about 120 mAh g^{-1} at a rate of 6*C* discharging) and smaller R_{ct}. The present synthesis condition is simply, easily controlled, and this method can be used to prepare high battery-active cathode material in a large scale.

2. Experimental

2.1. Synthesis

The sample was prepared from precursor $Ni_{1.5}Mn_{1.5}O_4$, which was prepared as follows. Mixture of $Mn(CH_3COO)_2{\cdot}4H_2O$ (AR, 99%) and $Ni(CH_3COO)_2.4H_2O$ (AR, 98%) were completely dissolved into distilled water with molar ratio of 1:1, water was removed by means of a rotary evaporator at 75 °C, and salt precipitate was made. The salt precipitate was ground and calcined at 800 °C for 12 h in air. The as-prepared precursor was mixed with $LiOH{\cdot}H_2O$ (AR, 95%) in stoichiometric proportions and pressed into pellet. The pellets were heated at 480 °C for 3 h in air followed by annealing at 800, 850 and 900 °C for 12 h, respectively. The pellets were quenched to the room temperature using a copper plate.

2.2. Characterization

Powder X-ray diffraction (XRD) was performed on a Philips X'pert pro X-ray diffractometer equipped with graphite monochromatized high-intensity Cu Kα radiation (λ = 1.54178) in the 2θ range from 10° to 80°. The contents of cations in both precursor and sample were measured by inductively coupled plasma atomic analysis (ICP, Atomscan Advantage). The scanning electron microscope (SEM) study of the samples was performed using JEOL JSM-6700F electron microscope.

2.3. Electrochemical characterization

Charge and discharge profiles were collected by galvanostatically cycling between 2.5 and 4.4 V on multi-channel battery testers (Shenzhen Neware, BTS, China). For the preparation of cathode sheets, slurry was formed by mixing the active material, acetylene black, and binder (polyvinylidene fluoride, PVDF, dissolved in *N*-methyl-2-pyrrolidone, NMP) in a weight ratio of 75:20:5. The slurry was spread uniformly on aluminum foil. The electrodes were dried under vacuum at 120 °C overnight and then punched and weighed. 1 M $LiPF_6$ in a 1:1 ethylene carbonate/diethyl carbonate was used as electrolyte, and lithium foil was used as anode. A thin sheet of microporous polypropylene insulated the cathode from lithium foil anode. Battery assembly was carried out in an argon-filled glove box. CV and electrochemical impedance spectroscopy (EIS) were measured on an electrochemical workstation (CHI660C, Shanghai, China). CV was carried out at a scanning rate of 0.1 mV s^{-1} between 2.5 and 4.4 V (vs. Li/Li^+). EIS was conducted in a frequency range from 0.1 MHz to 0.01 Hz using an ac signal with 5 mV amplitude. Impedance data were analyzed with ZView-Impedance Software.

3. Results and discussion

The chemical compositions of the prepared powders were determined by ICP and the results are summarized in Table 1. The measured cation ratios of Ni:Mn and Li:Ni:Mn are well in agreement to the intended composition, which implies that metal oxides are homogeneously reacted.

Table 1
Chemical composition (wt.%) of the prepared precursor and product determined by ICP

Li	Ni	Mn	Formula
–	34.42	32.60	$Ni_{1.48}Mn_{1.50}O_4$
6.51	27.47	25.65	$Li_{1.01}Ni_{0.5}Mn_{0.5}O_2$

Fig. 1a shows the XRD pattern of as-synthesized precursor $Ni_{1.5}Mn_{1.5}O_4$, which is similar to the pattern of $NiMn_2O_4$ with JCPDS card number 84–0542. All the peaks in Fig. 1a can be indexed to the *Fd*3*m* space group with a cubic lattice. The purpose of making $Ni_{1.5}Mn_{1.5}O_4$ is to ensure sufficient mixing of Mn–Ni in the precursor at the atomic level, and to obtain the pure phase $LiNi_{0.5}Mn_{0.5}O_2$. This technique route appears to be successful as the XRD pattern of the final product (Fig. 1b) can be indexed with the α-$NaFeO_2$-type structure ($R\bar{3}m$) with scarcely any sign of the unwanted Li_2MnO_3 phase. The inset in Fig. 1b is the magnified XRD pattern between 20° and 30°. No diffraction peak can be detected in this range, indicating that Li_2MnO_3-based oxide does not exist in the final sample under the detection limitation [10,13]. Lattice parameters obtained from ten $LiNi_{0.5}Mn_{0.5}O_2$ samples with the identical electrochemical reactivity are $a = 2.880\ (2)$ Å and $c = 14.26\ (1)$ Å in a hexagonal. Both the c/a ratio (4.95) and the I_{003}/I_{104} intensity ratio (1.46) indicate a high degree of Li–M (Ni, Mn) order in their respective layers [12,14]. The splitting of the (0 0 6)/(1 0 2) and (1 0 8)/(1 1 0) diffraction pairs can be clearly detected, indicating that the product of $LiNi_{0.5}Mn_{0.5}O_2$ is of almost ideal layered structure and crystallinity [11].

The ratio of I_{003}/I_{104} is sensitive to synthesis conditions. The ratio of I_{003}/I_{104} decreases with increasing heat-temperature up to 900 °C since the amount of Li/Ni disorder increases as the heating temperature increases [12]. While heat-temperature decreases to 800 °C, the sample with the smaller ratio of I_{003}/I_{104} contains impurity (Supporting Material, Fig. 1S). Electrochemical performance of both samples obtained at 800 and 900 °C is poor comparing to that obtained at 850 °C (Supporting material, Fig. 2S). In the following, we will focus our attention on the sample obtained at 850 °C.

The morphology of the precursor $Ni_{1.5}Mn_{1.5}O_4$ and the final sample $LiNi_{0.5}Mn_{0.5}O_2$ is shown in Fig. 2. The precursor has a uniform structural morphology and smooth crystal surface with narrow size distribution, which is less than 1 μm. The final sample has an irregular morphology, the size distribution is from submicron to micrometer.

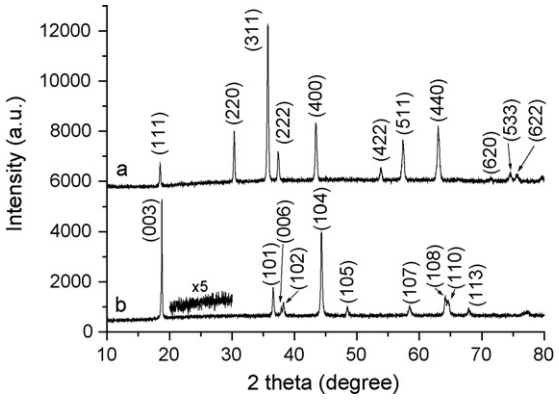

Fig. 1. XRD patterns of precursor $Ni_{1.5}Mn_{1.5}O_4$ (a) and $LiNi_{0.5}Mn_{0.5}O_2$ (b). The inset in the pattern (b) is magnified by 5 times.

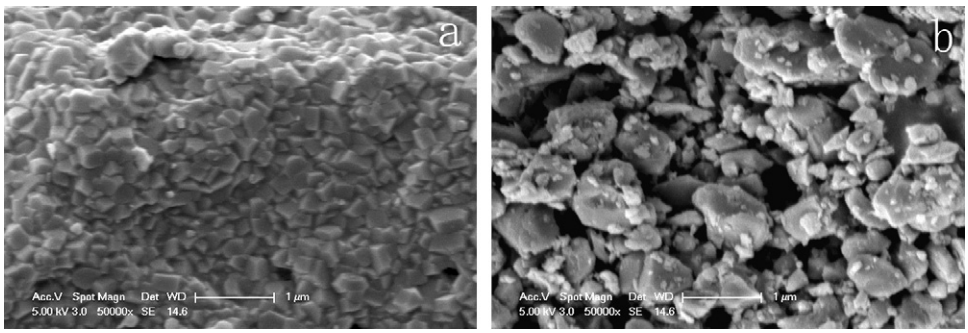

Fig. 2. SEM images of $Ni_{1.5}Mn_{1.5}O_4$ (a) and $LiNi_{0.5}Mn_{0.5}O_2$ (b).

In order to examine the electrochemical reactivity and stability of $LiNi_{0.5}Mn_{0.5}O_2$, 100 cycle tests were carried out at a specific rate of 21.7 mA g^{-1} at room temperature. As shown in Fig. 3(a), the first charge and discharge capacity were 207 and 199 mAh g^{-1}, respectively, the ratio of discharge/charge is about 96%. From the second to the one-hundredth cycle, the ratio of discharge/charge is larger than 99%, illuminating that electrochemical reversibility was established after the initial cycle. As shown in Fig. 3(b), the batteries show about 190 mAh g^{-1} of rechargeable capacity without dramatic capacity fading during 100 cycles, with only 4.7% capacity decreased after 100 cycles. This result indicates that the designed cathode material with high capability has a high degree of cation ordering required for good Li^+ mobility [15].

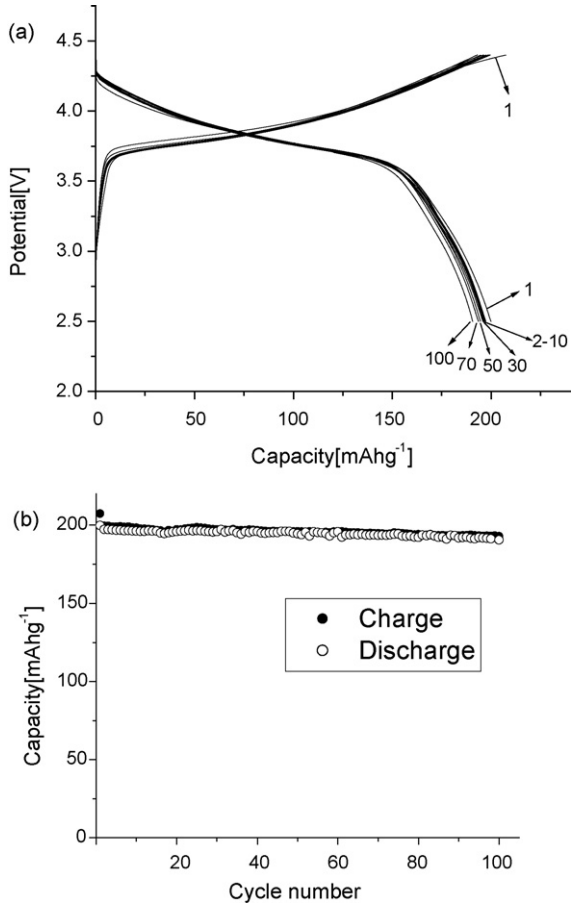

Fig. 3. (a) Galvanostatic cycles for a battery operated in the voltage range from 2.5 to 4.4 V at a rate of 21.7 mA g^{-1} and (b) charge and discharge capacities as a function of cycle number.

Fig. 4(a) shows the discharged curves at different discharged currents and Fig. 4(b) shows the results on high-rate capability tests accompanied with stability tests of a $Li/LiNi_{0.5}Mn_{0.5}O_2$ battery. In the calculation of *C*-rate, 190 mA g^{-1} is assumed to be roughly equivalent to 1*C*. Discharge currents varied from 47.6 to 1142.9 mA g^{-1} which corresponds to the rate from 0.25*C* to 6*C*, and 15 cycles were carried out at each different current. The battery was charged at the same specific current of 47.6 mA g^{-1} (0.25*C* rate) to ensure identical initial state for each discharge. As shown in Fig. 4(b), for each 15 cycles at the same rate, the rate capacities scarcely changed. Even after 15 cycles at the rate of 6*C*, 97.5% initial capacity (about 117.5 mAh g^{-1}) remained. The present result in this study is much better than that of SS-$Li(Ni_{0.5}Mn_{0.5})O_2$ prepared by solid-state reaction [7]. The ratio of I_{003}/I_{104} stands for cation ordering in their respective layers [12,14]. The ratio is about 1.74 for IE-$Li(Ni_{0.5}Mn_{0.5})O_2$ [12], 1.46 in this study and 1.26 for SS-$Li(Ni_{0.5}Mn_{0.5})O_2$ [12]. The corresponding capacity at almost same discharge rate (note: 4*C* in Ref. [7] is equal to 5.9*C* in this study) is ~180 mAh g^{-1} [7], 120 mAh g^{-1} and ~80 mAh g^{-1} [7], respectively. The relationship between the ratio and capacity is almost linear as shown in Fig. 5. The similar relationship has been found from another set of data from our group (Supporting material, Fig. 3S). Those facts suggest that the large capacity performance in the high-rate condition could be attributed to improved cation ordering. The capacity is still about 188 mAh g^{-1}, which is almost its original value, when the discharge rate returns to 47.6 mA g^{-1} after completion of the high rates test, indicating that the as-prepared $LiNi_{0.5}Mn_{0.5}O_2$ material has good electrochemical reversibility and structure stability. The high-rate discharge performance suggests that the synthesized $LiNi_{0.5}Mn_{0.5}O_2$ composite would be well suitable for cathode materials of high power lithium batteries.

CV of $LiNi_{0.5}Mn_{0.5}O_2$ sample was tested in the potential region of 2.5–4.4 V. As shown in Fig. 6, there are no redox peaks around 3 V in the CV curve, indicating that Mn ions are electrochemically inactive and present 4+ oxidation state in the sample. Therefore, the observed peaks near 4 V are attributed to the redox reaction of Ni^{2+}/Ni^{4+} according to Lu et al. and Kang et al. [16,17]. The oxidation and reduction peaks are located at around 4.00 V (φ_{ox}) and 3.71 V (φ_{red}), respectively, and the differential peak potential $\Delta\varphi$ between φ_{ox} and φ_{red} is about 0.29 V, which is smaller than 0.37 V reported by Kang et al. [17]. The smaller the differential redox potential is, the better the electrochemical reversibility is. The CV result indicates that our sample should be of better reversibility and charge–discharge performance, which is well agreement with the result of battery test.

To further understand the reason for the improved rate capability of $LiNi_{0.5}Mn_{0.5}O_2$ prepared from precursor $Ni_{1.5}Mn_{1.5}O_4$, EIS was carried out in pristine state, fully charged state to 4.4 V and fully discharged state to 2.5 V versus Li/Li^+. In order to keep the cell at the 4.4 V charged state, the cell was first charged at

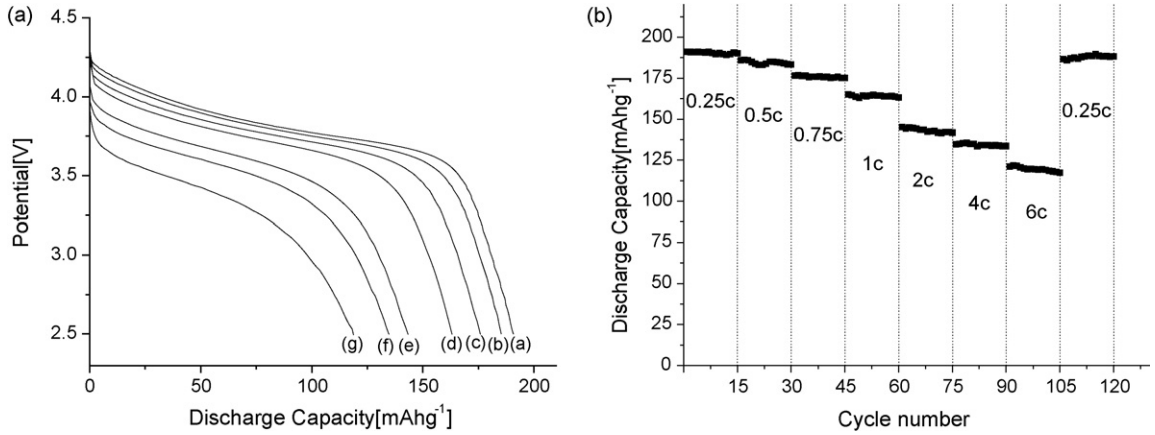

Fig. 4. (a) Discharge curves at different current densities. The assumed value of 1*C* is 190 mA g^{-1} here. (a) 0.25*C*, (b) 0.5*C*, (c) 0.75*C*, (d) 1*C*, (e) 2*C*, (f) 4*C*, and (g) 6*C*. (b) Discharge capacity at different current with cycle number. The charge rate was fixed at 0.25*C* (=47.6 mA g^{-1}).

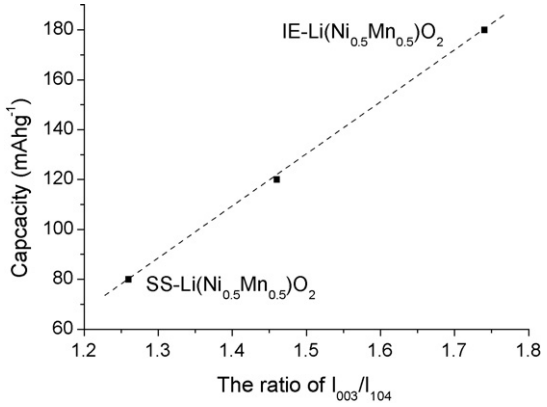

Fig. 5. The relationship between the ratio of I_{003}/I_{104} and capacity at the rate of 6*C*. The data of IE- and SS-Li($Ni_{0.5}Mn_{0.5}$)O_2 were from Ref. [7,12]. 4*C* discharging rate in Ref. [7] is equal to 5.9*C* in this study.

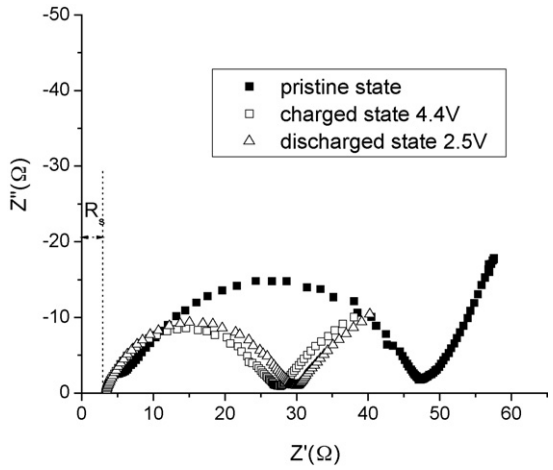

Fig. 7. Nyquist plots of $LiNi_{0.5}Mn_{0.5}O_2$ electrode in pristine state, fully charged state (4.4 V) and fully discharged state (2.5 V). EIS was conducted in a frequency range from 0.1 MHz to 0.01 Hz using an ac signal with 5 mV amplitude.

constant current to 4.4 V and then followed by constant voltage charge held at 4.4 V for another 10 h before the EIS data were collected. Nyquist plots of pristine state, charged state and discharged state of the Li-ion cell are shown in Fig. 7. Nyquist plot of pristine state consists of a high-frequency semicircle and a sloping line in the low-frequency region. As shown in Fig. 7, a resistance component R_e is arising from cell electrolyte resistant and cell component. The semicircle may be attributed to the lithium ion migration through the interface between the surface layer of the particles and the electrolyte as addressed by Aurbach et al. [18,19]. When the electrode was charged to 4.4 V, a semicircle and a half semicircle appeared in the plot. The resistance of the semicircle is obviously decreased to 22.4 Ω. The decrease in the impedance at the charged state could be due to destruction or modification of the inactive surface film covering the virgin electrode surface by the current flux [20,21]. A new semicircle (only a half semicircle observed due to the limitation of the machine) appeared in the low-frequency region, whose original could be assigned to the charge transfer resistance (R_{ct}) [20–23]. R_{ct} is about 42.1 Ω on the bases of fitting with ZView-Impedance Software. This value is obviously smaller than the R_{ct} of $LiNi_{0.5}Mn_{0.5}O_2$ synthesized by other methods [20,21]. After discharging to 2.5 V, no significant change was observed in the Nyquist plot comparing to the 4.4 V charged state, only the corresponding resistance slightly increases, which is coincident to the observations that the impedance of the cell in the fully charged state is lower than that in the fully discharged state [21,24].

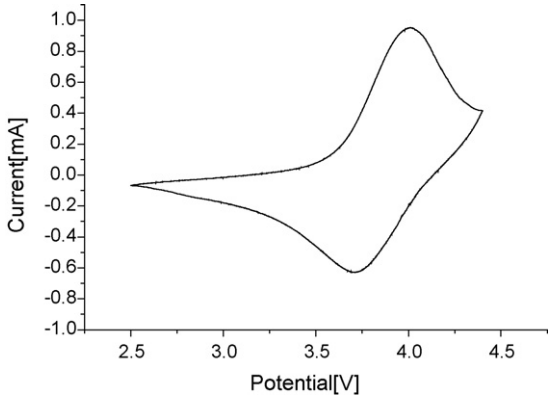

Fig. 6. Cyclic voltammetry of the synthesized $LiNi_{0.5}Mn_{0.5}O_2$ in the voltage range 2.5–4.4 V at scanning rate 0.1 mV s^{-1}.

4. Conclusion

The solid solution of $Ni_{1.5}Mn_{1.5}O_4$ is a good precursor to fabricate high battery-active $LiNi_{0.5}Mn_{0.5}O_2$ cathode material since the distribution of nickel and manganese is homogeneous at atomic level in the solid solution, which results in highly ordering of cations

and no structural impurity in the final sample $LiNi_{0.5}Mn_{0.5}O_2$. The present synthesis condition is simply, easily controlled, and this method can be used to prepare high battery-active cathode material in a large scale. The electrochemical performance indicates that $LiNi_{0.5}Mn_{0.5}O_2$ prepared in this study has a competitive capacity, cycle ability and discharge rate since this cathode material is of better electrochemical reversibility and smaller resistance of charge transfer. The data from literatures and our group indicate that $LiNi_{0.5}Mn_{0.5}O_2$ can be used as a possible alternative to $LiCoO_2$ in response to an expanding need for the advanced lithium-ion batteries.

Acknowledgment

This work was supported by the foundation of Department of Science and Technology, Anhui province.

Appendix A. Supplementary data

Supplementary data associated with this article can be found, in the online version, at doi:10.1016/j.jpowsour.2008.04.015.

References

[1] J.-M. Tarascon, M. Armand, Nature 414 (1998) 359–367.
[2] Y. Xia, H. Takeshige, H. Noguchi, M. Yoshio, J. Power Sources 56 (1995) 61–67.
[3] Z. Liu, W.-L. Wang, X. Liu, M. Wu, D. Li, Z. Zhen, J. Solid State Chem. 177 (2004) 1585–1591.
[4] A.K. Padhi, K.S. Nanjundaswamy, J.B. Goodenough, J. Electrochem. Soc. 144 (1997) 1188–1194.
[5] T. Ohzuku, Y. Makimura, Chem. Lett. (2001) 744–745.
[6] Y. Makimura, T. Ohzuku, J. Power Sources 119–121 (2003) 156–160.
[7] K. Kang, Y.S. Meng, J. Breger, C.P. Grey, G. Ceder, Science 311 (2006) 977–980.
[8] Z. Lu, D.D. MacNeil, J.R. Dahn, Electrochem. Solid-State Lett. 4 (2001) A191–A194.
[9] Z. Lu, L.Y. Beaulieu, R.A. Donaberger, C.L. Thomas, J.R. Dahn, J. Electrochem. Soc. 149 (2002) A778–A791.
[10] J. Cho, Y. Kim, G. Kim, J. Phys. Chem. C 111 (2007) 3192–3196.
[11] B. Zhang, G. Chen, P. Xu, Z. Lv, Solid State Ionics 178 (2007) 1230–1234.
[12] Y. Hinuma, Y.S. Meng, K. Kang, G. Ceder, Chem. Mater. 19 (2007) 1790–1800.
[13] Y.J. Park, Y.-S. Hong, X. Wu, M.G. Kim, K.S. Ryu, S.H. Chang, J. Electrochem. Soc. 151 (2004) A720–A727.
[14] M. Yoshio, Y. Todorov, K. Yamato, H. Noguchi, J. Itoh, M. Okada, T. Mouri, J. Power Sources 74 (1998) 46–53.
[15] B. Schougaard, J. Breger, M. Jiang, C.P. Grey, J.B. Goodenough, Adv. Mater. 18 (2006) 905–909.
[16] Z.H. Lu, L.Y. Beaulileu, R.A. Donaberger, C.L. Thomas, J. Electrochem. Soc. 149 (2002) A778–A791.
[17] S.-H. Kang, J. Kim, M.E. Stoll, D. Abraham, Y.K. Sun, K. Amine, J. Power Sources 112 (2002) 41–48.
[18] D. Aurbach, M.D. Levi, E. Levi, H. Teller, B. Markovsky, G. Salitra, U. Heider, L. Heider, J. Electrochem. Soc. 145 (1998) 3024–3034.
[19] M.D. Levi, G. Salitra, B. Markovsky, H. Teller, D. Aurbach, U. Heider, L. Heider, J. Electrochem. Soc. 146 (1999) 1279–1289.
[20] B. Markovsky, D. Kovacheva, Y. Talyosef, M. Gorava, J. Grinblat, D. Aurbach, Electrochem. Solid-State Lett. 9 (2006) A449–A453.
[21] K.M. Shaju, G.V.S. Rao, B.V.R. Chowdari, Electrochim. Acta 49 (2004) 1565–1576.
[22] B. Lin, Z. Wen, Z. Gu, S. Huang, J. Power Sources 175 (2008) 564–569.
[23] D. Li, Y. Sasaki, K. Kobayakawa, Y. Sato, Electrochim. Acta 51 (2006) 3809–3813.
[24] G. Ning, B. Haran, B.N. Popov, J. Power Sources 117 (2003) 160–169.